Evaluating a Semi-continuous Multi-compartmental Intra-Voxel Incoherent Motion (IVIM) Model in the Brain: How Does the Method Influence the Results in IVIM?

Vera Catharina Keil[1], Burkhard Maedler[2], Hans Heinz Schild[1], and Dariusch Reza Hadizadeh[1]
[1]*Radiology, UK Bonn, Bonn, NRW, Germany,* [2]*Radiology MRI Unit, PHILIPS Healthcare, Hamburg, Germany*

Target Audience: This study is particularly interesting for scientists and clinicians experimenting with IVIM and other quantitative diffusion methods to gain better insights into the understanding of IVIM methods and critically consider their shortcomings.

Purpose: Comparison of a novel semi-continuous non-negative least squares diffusion model with classic mono-and bi-exponential methods for CNS applications.

Introduction: LeBihan's model for intra-voxel incoherent motion (IVIM) analysis of diffusion-weighted MRI (DWI) data proposes a possibility to separate intra- and extracellular diffusion from intracapillary motion of water molecules [1,2]. IVIM may reveal the full grade of water diffusion restriction and additionally be a non-invasive tool to generate maps of tissue microperfusion. The method is vulnerable to motion and pulsation artefacts [3]. Further, the deconvolution of the complex multi-exponential process of water diffusion is an on-going topic of scientific discussion resulting in multiple methods of diffusion curve fitting and a dispute over the nature of microperfusion [4]. Yet, publications for clinical IVIM applications in the brain, an organ with particularly anisotropic diffusion properties, are recently on the rise. Suggestions to compare IVIM perfusion fractions with other perfusion techniques are attempted [5,6]. We compared a novel semi-continuous approach to two established methods and to a macrovascular perfusion technique in order to reveal their impact on the results.

Methods: 30 patients with different cerebral lesions and 9 control subjects (Table 1) were examined with a 3T MRI (Philips Achieva TX; Dual Nova gradients 80 mT/m, 200 T/(m x s), whole-brain single shot isotropically weighted DWI sequence: 36 slices, 116 x 112 matrix, 2 mm³ voxel size, three orthogonal gradient directions (x,y,z), TR=4.1s, TE=66ms, 32 b-values (0 to 2000 s/mm² with a higher sampling density at low b-values, image registration: b=0, eddy-current correction), scan time 6.3 min) [7]. ROI- and voxel-based data analyses were performed with a regularized NNLS (non-negative least squares) algorithm for the corresponding diffusion signal kernel (101 log-spaced coef. from 0.1 to 1000 µm²/ms). Diffusion distribution spectra ("D") were obtained from a pixel-by-pixel analysis derived from any apparent diffusion coefficient (ADC) ([7] and Fig.1). This semi-continuous approach delivers quantitative diffusion fraction (Df) maps, geometric mean diffusivity (gmD) and allows calculating the intravascular perfusion fraction (vPF; Fig 2). As a methodological comparison, all cases received mono- and bi-exponential IVIM vPF and ADC evaluations [8]. In tumors with hyperperfusion T1-DCE MRI sequences were acquired with transfer constant (K_{trans}) representing a perfusion parameter (Gadovist (Bayer Healthcare) i.v., 0.1 mmol/kg body weight; 50 dynamic scans, 36 slices, TR=3.5 ms, TE=1.7 ms, voxel size 1.57 x 1.6 x 3.0 mm, scan time 5.3 min). ROI-based vPF were compared to their K_{trans} counterparts.

Results: 1) Even in contrast-enhancing tumors (e. g. glioblastoma), vPF was very small (below 6.0% vs. 3.0% in healthy controls). Particularly near CSF spaces vPF was regularly overestimated (increase of vPF up to 400%). In comparison, vPF was 5.3x larger when applying a bi-exponential compared to a mono-exponential approach and less variable: smaller variance histogram (0.96±0.54 (mono) vs. 0.47±0.13 (bi)). NNLS-modelling allowed similarly high vPF values when choosing a D-range close to free water, otherwise NNLS-vPF was lower. 2) In contrast-enhancing regions vPF and ADC did not correlate with histology (e.g. glioblastoma vs. meningioma). Neither could non-enhancing tumors, scar tissue and multiple sclerosis lesions be differentiated from edema by any of the IVIM protocols. vPF nevertheless was highest in contrast-enhancing regions , less in necrosis, and equal to healthy tissue in signal elevated regions of T2w images. 3) K_{trans} and vPF did not significantly correlate.

Discussion and Conclusion: Inconsistent vPF for mono- and bi-exponential IVIM in regions of elevated motion (pulsatile vessel and CSF flow, pulsation of cortical brain) suggest that these methods are prone to overestimate non-coherent microperfusion due to their susceptibility to coherent motion and pulsation. As the integration window of our continuous NNLS-method can be set at any level, it is possible to create very similar vPF-maps compared to bi-exponential IVIM, if the D-range is chosen very close to D of free water (3 µm²/ms). This may explain the overestimation of bi-expontential vPF due to contamination of diffusion processes. The NNLS-approach can clearly separate those processes and allows a better characterisation of the complex diffusion processes in the brain. Additionally, mono- and bi-exponential least squares fitting methods will inherently produce biased results due to their incapability to address the ill-posed nature of multi-exponential decay at low SNR. Lacking correlation between vPF and K_{trans} suggests that IVIM microperfusion is different from macrovascular perfusion. It is doubtful if IVIM can be used for tumor differentiation.

Patient Collective (Table 1)	
Entity	**Number of Patients**
Glioma/Gliosis	
Glioblastoma (WHO °IV)	8
Astrocytoma (WHO °III)	2
Astrocytoma (WHO °II)	2
Post-traumatic scar tissue	1
Meningioma	
WHO °III	1
WHO °II	2
WHO °I	9
Cerebral Metastases	3
Multiple Sclerosis	1
Vascular Neoplasia	1
Healthy Control Patients	9
Total patient number	**39**

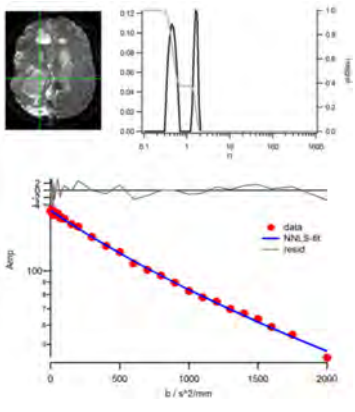

Fig.1: A multi-b decay curve (bottom) from one pixel of a malignant tumor and its diffusion spectrum (top right).

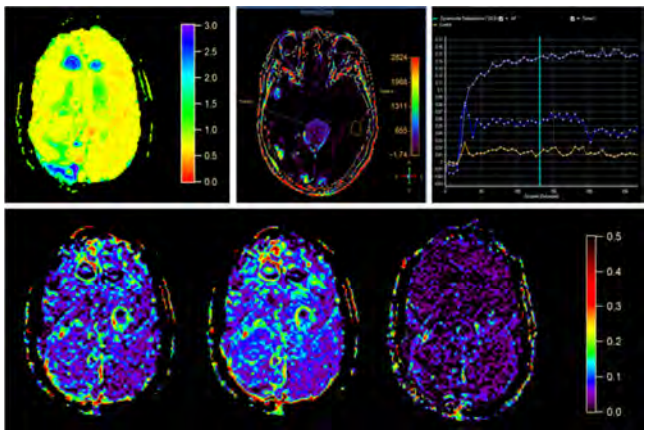

Fig.2: Examples of parameter maps: ADC (top left), K_{trans} and dynamic contrast curves (top right, different slice position), bottom: vPF classic mono-exp IVIM (left), bi-exp (middle), reg-NNLS (right).

References: *[1] Le Bihan D et al.: Radiology, 1988; 168(2):497-505; [2] Le Bihan D: MRM, 1990;14(2):283-92; [3] Kwong KK et al.: MRM, 1995; 21: 157–163.; [4]Henkelman M: MRM, 1990; 16,470-475; [5] Suh CH et al.: Radiology, 2014; 272:2,504-513; [6] Federau C et al.: JMRI, 2014; 39, 624–632; [7] Mädler B et al.: ISMRM 2013; # 5563; [8] Senegas J et al.: ISMRM 2014; #131.*